

# A Theoretical Study of the Reaction of $\text{HCO}^+$ with $\text{C}_2\text{H}_2$

E. DEL RÍO, R. LÓPEZ, M. I. MENÉNDEZ, T. L. SORDO

*Departamento de Química Física y Analítica, Facultad de Química, Universidad de Oviedo, C/ Julián Clavería, 8, 33006 Oviedo, Principado de Asturias, Spain*

*Received 9 June 1999; accepted 9 August 1999*

**ABSTRACT:** A theoretical study was performed for the reaction of formyl cation and acetylene to give  $\text{C}_3\text{H}_3^+ + \text{O}$  in flames and  $\text{C}_2\text{H}_3^+$  (nonclassical) + CO, both in flames and in interstellar clouds. The corresponding Potential Energy Surface (PES) was studied at the B3LYP/cc-pVTZ level of theory, and single-point calculations on the B3LYP geometries were carried out at the CCSD(T)/cc-pVTZ level. Our results display a route to propynal evolving energetically under  $\text{C}_2\text{H}_3^+$  (nonclassical) + CO and, consequently, accessible in interstellar clouds conditions. This route connects the most stable  $\text{C}_3\text{H}_3\text{O}^+$  isomer (C2-protonated propadienone) with a species from which propynal may be produced in a dissociative electron recombination reaction. The reaction channel to produce the  $\text{C}_3\text{H}_3^+ + \text{O}$  evolves basically through two TSs and presents an endothermicity of 63.9 kcal/mol at 2000 K. According to our Gibbs energy profiles, the C2-protonated propadienone is the most stable species at low-moderate temperatures and, consequently, could play a certain role in interstellar chemistry. On the contrary, in combustion chemistry conditions (2000 K) the  $\text{C}_2\text{H}_3^+$  (nonclassical) + CO products are the most thermodynamically favored species. © 2000 John Wiley & Sons, Inc. *J Comput Chem* 21: 35–42, 2000

**Keywords:** ab initio calculations; hydrocarbon flames; interstellar chemistry; reaction channels; thermodynamic analysis

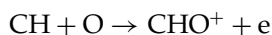
Correspondence to: Tomás L. Sordo; e-mail: [tsg@dwarf1.QUIMICA.UNIOVI.ES](mailto:tsg@dwarf1.QUIMICA.UNIOVI.ES)

Contract/grant sponsor: FICYT (Spain); contract/grant number: PB-AMB98-05C1

Contract/grant sponsor (to E. del R.): DGEISIC

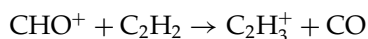
## Introduction

The formyl cation  $\text{HCO}^+$  is present in flames,<sup>1</sup> plasmas,<sup>2</sup> and in the interstellar clouds.<sup>3</sup> In fact, it is generally agreed<sup>4,5</sup> that reaction



is the primary source of ionization in hydrocarbon flames. Among the positive ion–molecule reactions considered to play a role in hydrocarbon flame ionization are those between  $\text{CHO}^+$  ions and  $\text{H}_2\text{O}$ ,  $\text{CH}_2$ ,  $\text{C}_2\text{H}_2$ , and  $\text{NH}_3$ .<sup>6,7</sup> The mechanisms for the reactions of  $\text{CHO}^+$  with  $\text{CH}_2$ ,  $\text{H}_2\text{O}$ , and  $\text{NH}_3$  have already been theoretically studied by our group.<sup>8,9</sup>

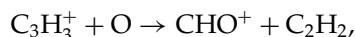
Vinckier et al.<sup>10</sup> found in acetylene rich systems with O atoms that the reaction



was the first step for ionic polymerization with acetylene to form  $\text{C}_{2n}\text{H}_{2n-1}^+$  and  $\text{C}_{2n}\text{H}_{2n+1}^+$ , which they suggested to be the nucleation centers for soot formation in fuel rich flames.

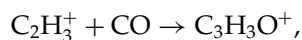
$\text{CHO}^+$  and  $\text{C}_2\text{H}_2$  can also react to produce an oxygen atom and  $\text{C}_3\text{H}_3^+$ , the dominant ion observed

in fuel rich flames. Reaction enthalpy for the reverse process,

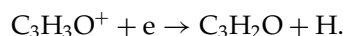


has been reported to be  $-67 \text{ kcal/mol}$ .<sup>6</sup>

On the other hand, the combination of  $\text{CHO}^+$  and  $\text{C}_2\text{H}_2$  leads to  $\text{C}_3\text{H}_3\text{O}^+$  ions, some of which have been characterized both experimentally<sup>11,12</sup> and theoretically.<sup>13,14</sup> It has been postulated<sup>15</sup> that interstellar propynal is formed by the association reaction



followed by the dissociative electron recombination reaction



Theoretical calculations<sup>14</sup> and SIFT experiments<sup>12</sup> show that the reaction of  $\text{C}_2\text{H}_3^+$  and CO forms C2-protonated propadienone, which would not yield propynal in a dissociative electron recombination reaction. Further, any rearrangement of C2-protonated propadienone to form an ion that would give propynal in a dissociative electron recombination reaction is not possible under the conditions

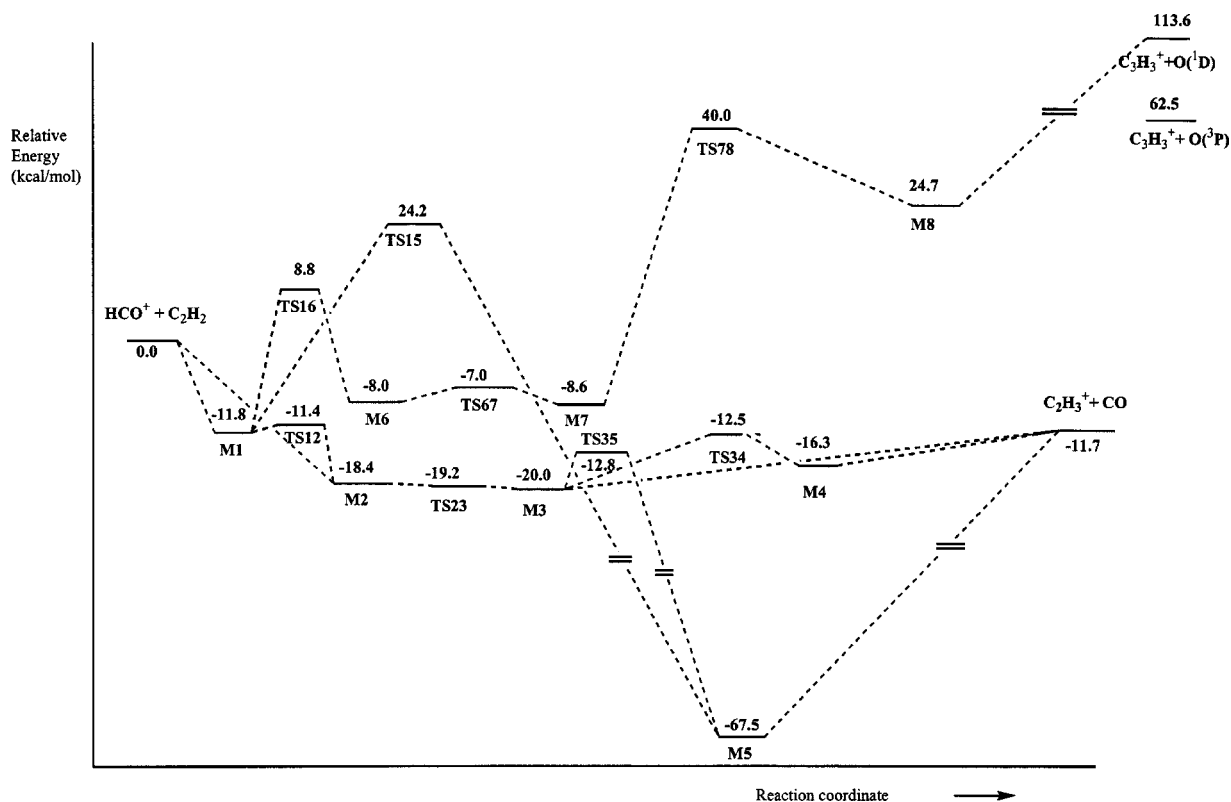


**FIGURE 1.** CCSD(T)/cc-pVTZ//B3LYP/cc-pVTZ energy profile including the ZPVE correction for the reaction between  $\text{HCO}^+$  and  $\text{C}_2\text{H}_2$ .

of interstellar clouds, given that it would involve a transition state (TS) higher in energy than  $\text{C}_2\text{H}_3^+ + \text{CO}$ .<sup>14</sup>

The aim of the present work is to theoretically study the mechanism of the title reaction to produce  $\text{C}_3\text{H}_3^+ + \text{O}$  in flames and  $\text{C}_2\text{H}_3^+ + \text{CO}$  both in flames and in interstellar clouds, focusing our attention on the elucidation of the formation of the interstellar propynal.

## Methods

Quantum chemical calculations were performed with the GAUSSIAN 94 series of programs.<sup>16</sup> Stable species were fully optimized and TSs located using Schlegel's algorithm<sup>17</sup> at the B3LYP/cc-pVTZ theory level.<sup>18</sup> All the critical points were further characterized and the zero-point vibrational energies (ZPVEs) were evaluated by analytical computations of harmonic vibrational frequencies at the

B3LYP/cc-pVTZ level. Single-point calculations on the B3LYP/cc-pVTZ geometries were also carried out at the CCSD(T)/cc-pVTZ level.

Intrinsic Reaction Coordinate (IRC) calculations starting at each saddle point verified the two minima connected by that TS using the Gonzalez and Schlegel method<sup>19</sup> implemented in GAUSSIAN 94.

$\Delta H$ ,  $\Delta S$ , and  $\Delta G$  values were also calculated to obtain results more readily comparable with experiment within the ideal gas, rigid rotor, and harmonic oscillator approximations.<sup>20</sup> A pressure of 1 atm and 100, 298.15, and 2000 K of temperature were assumed in the calculations.

## Results and Discussion

Figure 1 presents the CCSD(T)/cc-pVTZ//B3LYP/cc-pVTZ energy profiles corresponding to the reaction of  $\text{HCO}^+$  with  $\text{C}_2\text{H}_2$ . Figure 2 collects the optimized critical structures appearing in

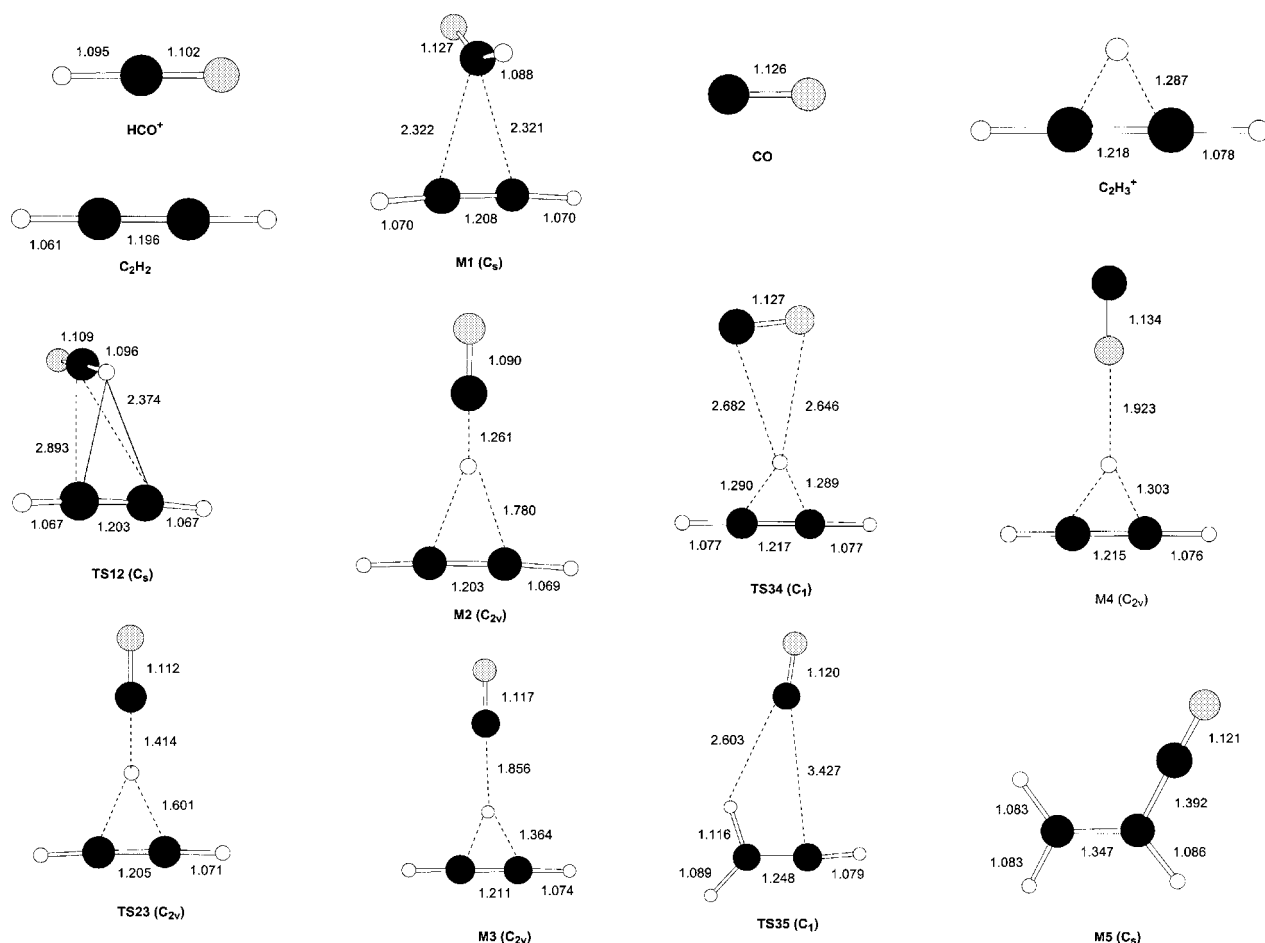


**FIGURE 2.** B3LYP/cc-pVTZ optimized critical structures located along the energy profile for the reaction between  $\text{HCO}^+$  and  $\text{C}_2\text{H}_2$ . Distances are given in angstroms.

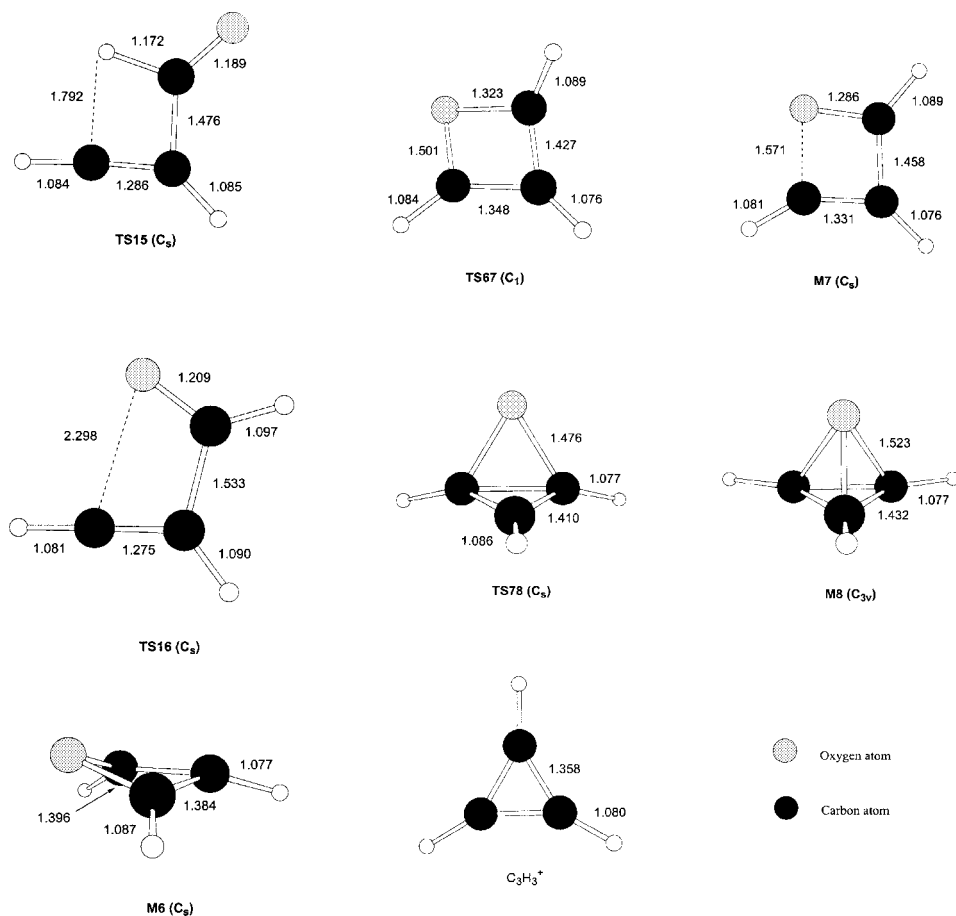


FIGURE 2. (Continued)

Figure 1. Table I presents the absolute and relative energies of the critical structures at B3LYP/cc-pVTZ and CCSD(T)/cc-pVTZ//B3LYP/cc-pVTZ levels. Unless otherwise indicated, we will present in the text the CCSD(T) relative energies including the B3LYP ZPVE corrections.

The formyl cation can approach acetylene through the carbon atom or through the hydrogen atom, rendering the intermediates **M1** and **M2**, respectively. Both of them are connected by the TS **TS12**, as can be seen in Figure 1. **M2** evolves to the intermediate **M3** through the TS **TS23**. Three different reaction paths proceed under reactants energy from **M3** to the products  $C_2H_3^+$  (nonclassical) + CO (see Fig. 1). Along the first one, **M3** evolves directly, without any energy barrier, to give the products. The second path goes through a TS, **TS34**, to give the intermediate **M4**, which in turn, can lead directly to the products. The last one leads to the most stable intermediate, **M5**, through the TS **TS35**. **M5** can render the same products through a monotonously increasing profile.

At **M1**, the formyl cation is located perpendicular to acetylene forming a three-center interaction between the C atom of  $HCO^+$  and the two C atoms of  $C_2H_2$ . Both C(formyl)—C(acetylene) distances are about 2.32 Å, and the formyl fragment has lost its linearity presenting an H—C—O angle of 148.1°. The net NBO<sup>21</sup> charge transfer from the HOMO of  $C_2H_2$  to the LUMO of  $HCO^+$  is 0.31 e. **M1** is 11.8 and 0.1 kcal/mol more stable than isolated reactants and  $C_2H_3^+$  (nonclassical) + CO, respectively. **TS12**, which has  $C_s$  symmetry, is 0.4 kcal/mol above **M1**. In **TS12**, the  $HCO^+$  moiety is placed on the symmetry plane with the H and C atoms at 2.374 and 2.893 Å from acetylene C atoms, respectively. The net NBO charge transfer from acetylene amounts to 0.11 e. **M2** is 18.4 kcal/mol more stable than separate reactants. In **M2**, the  $HCO^+$  fragment remains linear with the H—C bond only slightly stretched ( $d(H—C) = 1.261$  Å) and the H atom situated in front of the middle point of the C—C bond in the acetylene molecule, but still far from it ( $d(H_{\text{formyl}}—C_{\text{acetylene}}) = 1.780$  Å (see Fig. 2). At **M2**, the net

TABLE I.

Absolute Energies (Hartree), Zero-Point Vibrational Energy Corrections (ZPVE) and Relative Energies (kcal/mol) for Chemically Important Structures Located on the Reaction of  $\text{HCO}^+$  with  $\text{C}_2\text{H}_2$ .

Species	Absolute Energy			Relative Energy	
	B3LYP/cc-pVTZ	CCSD(T)/cc-pVTZ //B3LYP/cc-pVTZ	ZPVE	B3LYP/cc-pVTZ	CCSD(T)/cc-pVTZ //B3LYP/cc-pVTZ
$\text{HCO}^+ + \text{C}_2\text{H}_2$	−190.95562	−190.57929	26.1	0.0	0.0
<b>M1</b>	−190.98651	−190.60149	28.2	−19.4	−13.9
<b>M2</b>	−190.98815	−190.60814	25.8	−20.4	−18.1
<b>M3</b>	−190.98942	−190.61029	25.6	−21.2	−19.5
<b>M4</b>	−190.98241	−190.60424	25.5	−16.8	−15.7
<b>M5</b>	−191.08157	−190.69592	31.8	−79.0	−73.2
<b>M6</b>	−190.98223	−190.59985	31.0	−16.7	−12.9
<b>M7</b>	−190.98203	−190.60111	31.2	−16.6	−13.7
<b>M8</b>	−190.92578	−190.54692	30.5	18.7	20.3
<b>TS12</b>	−190.97919	−190.59920	27.2	−14.8	−12.5
<b>TS23</b>	−190.98786	−190.60715	24.4	−20.2	−17.5
<b>TS34</b>	−190.97507	−190.59729	24.9	−12.2	−11.3
<b>TS35</b>	−190.98073	−190.59852	25.4	−15.8	−12.1
<b>TS15</b>	−190.93134	−190.54347	27.8	15.2	22.5
<b>TS16</b>	−190.95460	−190.56899	28.4	0.6	6.5
<b>TS67</b>	−190.98033	−190.59760	30.6	−15.5	−11.5
<b>TS78</b>	−190.90386	−190.52113	29.6	32.5	36.5
$\text{C}_2\text{H}_3^+ + \text{CO}$	−190.97402	−190.59553	24.6	−11.5	−10.2
$\text{C}_3\text{H}_3^+ + \text{O}(^1\text{D})$	−190.76402	−190.40183	28.3	120.2	111.4
$\text{C}_3\text{H}_3^+ + \text{O}(^3\text{P})$	−190.86564	−190.48320	28.3	56.5	60.3

NBO charge transfer from acetylene to the formyl cation is 0.22 e. The barrier to get **TS23** is only of 0.6 kcal/mol if ZPVE correction is not considered, and disappears when this correction is included (**TS23** is 19.2 kcal/mol under reactants). At **TS23** the proton is situated in front of the middle point of the C—C bond in acetylene at a distance of 1.414 Å from the C atom of CO and 1.601 Å from each acetylenic carbon atom. The net NBO charge transfer to the  $\text{HCO}^+$  moiety amounts to 0.33 e. Finally, at **M3**, the proton transfer is completed with distances of 1.856 and 1.364 Å from the proton to the C atom of CO and to the carbon atoms of acetylene, respectively (see Fig. 2). In **M3**, there is a  $\pi$  interaction between the HOMO of the acetylenic moiety and the next LUMO of the  $\text{HCO}^+$  fragment. As the next LUMO of  $\text{HCO}^+$  has antibonding character between the C atom and the H and O atoms, this interaction determines a slight elongation of the C—O bond and a much larger stretching of the C—H bond, the proton being practically transferred to the acetylene fragment. **M3** is 20.0 kcal/mol more stable than separate reactants.

As already mentioned, **M3** can follow three different pathways. It can dissociate along a  $\text{C}_{2v}$  path to yield the proton transfer products  $\text{C}_2\text{H}_3^+$  (nonclassical) + CO, 11.8 kcal/mol more stable than isolated reactants. Alternatively, the CO moiety in **M3** can rotate through the TS **TS34** with an energy barrier of 7.5 kcal/mol to give **M4** in which the  $\text{C}_2\text{H}_3^+$  (nonclassical) moiety interacts with the O atom of the CO fragment through the bridged H atom with an O—H distance of 1.923 Å (see Fig. 2). Acetylenic carbons are at 1.303 Å from the proton. **M4** is 16.3 kcal/mol more stable than separate reactants, and can lead to the products  $\text{C}_2\text{H}_3^+$  (nonclassical) + CO without any energy barrier. Finally, **M3** can evolve to **M5** through **TS35** with an energy barrier of 7.2 kcal/mol. In **TS35**, the proton of the  $\text{C}_2\text{H}_3^+$  moiety interacts in a  $\sigma$  fashion with one of the C atoms at a distance of 1.116 Å, whereas the CO fragment is starting to interact with the other C atom at a distance of 3.427 Å (see Fig. 2). **M5** is C2-protonated propadienone, which is the most stable structure located 67.5 kcal/mol under reactants.

Other routes from  $\text{HCO}^+ + \text{C}_2\text{H}_2$  to  $\text{C}_2\text{H}_3^+$  (non-classical) + CO pass through **M1**, the high-energy TS **TS15**, and the very stable intermediate **M5**. From **M5**, these routes can join the reaction paths previously described at the **M3** intermediate after passing the TS **TS35** (see Fig. 1), or directly lead to the proton transfer products. In **TS15**, which is 24.2 kcal/mol above isolated reactants, all atoms lie on a plane. A C(formyl)—C(acetylene) bond is practically formed with a distance of 1.476 Å, whereas the H atom of the cationic moiety, which is in an inward position, has started to detach from the C atom of the formyl fragment and to interact with the other C atom of acetylene. The formyl fragment presents an H—C—O angle of 118.6° (see Fig. 2). The important amount of energy required to reach **TS35** from **M5**, 54.7 kcal/mol, is due to the rupture of the C(formyl)—C(acetylene) bond.

The intermediate **M1**, already described, can also evolve through the TS **TS16** to give the four-membered  $\text{C}_3\text{H}_3\text{O}^+$  heterocycle **M6**. The main geometrical difference between **TS16** and **TS15** is the orientation of the formyl moiety: in **TS16**, the oxy-

gen atom is oriented inwards, whereas in **TS15**, it is oriented outwards. At **TS16**, one C(formyl)—C(acetylene) bond is formed, with a bond distance of 1.533 Å, and the formyl fragment is bent with an H—C—O angle of 126.4°. **TS16** is 15.4 kcal/mol more stable than **TS15**. **M6**, which has  $C_s$  symmetry (see Fig. 2) and is 8.0 kcal/mol more stable than separate reactants, is connected with a planar intermediate structure **M7** through the TS **TS67**, with a small energy barrier of only 1.0 kcal/mol. At **M7**, one of the C—O bonds has stretched to 1.571 Å, whereas the other one has shortened to 1.286 Å. The C—C bond next to the stretched C—O bond has shortened to 1.331 Å, and the C—C bond close to the shortened C—O bond has elongated to 1.458 Å. **TS67** has  $C_1$  symmetry and presents the same bond pattern as **M7**, although less pronounced. **M7** can evolve to an intermediate **M8**, 24.7 kcal/mol above reactants, through the TS **TS78** 40.0 kcal/mol less stable than reactants. **TS78** has  $C_s$  symmetry and corresponds to the displacement of the oxygen atom out of the molecular plane in **M7** to symmetrically interact with the two neighboring C atoms, which in turn, have approach each other

**TABLE II.** Enthalpies ( $\Delta H$ ), Entropy Contributions ( $-T\Delta S$ ) and Gibbs' Free Energies ( $\Delta G$ ) in kcal/mol for Chemically Important Structures Located on the Reaction of  $\text{HCO}^+$  with  $\text{C}_2\text{H}_2$  at 100, 298.15, and 2000 K.

Species	100 K			298.15 K			2000 K		
	$\Delta H$	$-T\Delta S$	$\Delta G$	$\Delta H$	$-T\Delta S$	$\Delta G$	$\Delta H$	$-T\Delta S$	$\Delta G$
$\text{HCO}^+ + \text{C}_2\text{H}_2$	0.0	0.0	0.0	0.0	0.0	0.0	0.0	0.0	0.0
<b>M1</b>	-12.3	0.5	-11.8	-12.4	1.7	-10.7	-8.1	2.8	-5.3
<b>M2</b>	-18.9	0.5	-18.4	-18.9	1.7	-17.2	-13.4	0.2	-13.2
<b>M3</b>	-20.5	0.5	-20.0	-20.4	1.4	-19.0	-14.8	-1.9	-16.7
<b>M4</b>	-16.7	0.3	-16.4	-16.4	0.4	-16.0	-10.9	-8.9	-19.8
<b>M5</b>	-68.2	0.9	-67.3	-69.1	4.2	-64.9	-67.0	27.7	-39.3
<b>M6</b>	-8.7	1.0	-7.7	-9.9	5.0	-4.9	-7.3	32.0	24.7
<b>M7</b>	-9.4	1.0	-8.4	-10.5	4.8	-5.7	-7.9	30.8	22.9
<b>M8</b>	23.9	1.0	24.9	22.7	5.2	27.9	25.9	31.6	57.5
<b>TS12</b>	-12.0	0.5	-11.5	-12.2	1.9	-10.3	-10.7	10.1	-0.6
<b>TS23</b>	-19.7	0.5	-19.2	-19.8	1.9	-17.9	-17.0	7.0	-10.0
<b>TS34</b>	-12.7	-0.2	-12.9	-12.6	-0.9	-13.5	-10.4	-10.7	-21.1
<b>TS35</b>	-13.2	0.2	-13.0	-13.0	0.3	-12.7	-11.0	-1.8	-12.8
<b>TS15</b>	23.5	0.9	24.4	22.6	4.3	26.9	23.3	30.0	53.3
<b>TS16</b>	8.1	0.9	9.0	7.2	4.0	11.2	7.8	28.6	36.4
<b>TS67</b>	-7.7	1.0	-6.7	-9.1	5.3	-3.8	-9.8	41.2	31.4
<b>TS78</b>	39.3	1.0	40.3	37.9	5.3	43.2	38.0	38.8	76.8
$\text{C}_2\text{H}_3^+ + \text{CO}$	-11.8	-2.2	-14.0	-11.8	-6.6	-18.4	-11.2	-45.1	-56.3
$\text{C}_3\text{H}_3^+ + \text{O}(^1\text{D})$	113.4	-1.6	111.8	112.9	-3.9	109.0	115.0	-27.8	87.2
$\text{C}_3\text{H}_3^+ + \text{O}(^3\text{P})$	62.3	-1.8	60.5	61.8	-4.5	57.3	63.9	-32.2	31.7

from a distance of 1.903 Å at **M7** to 1.491 Å. The intermediate **M8** has  $\text{C}_{3v}$  symmetry and presents the oxygen atom interacting with the three carbon atoms at a distance of 1.523 Å, the  $\text{C}_3\text{H}_3^+$  moiety lying on a plane (see Fig. 2). From **M8**, an oxygen atom can be directly eliminated to give cycle  $\text{C}_3\text{H}_3^+ + \text{O}(^1\text{D})$  113.5 kcal/mol above reactants.  $\text{O}(^3\text{P})$  is 51.0 kcal/mol more stable than  $\text{O}(^1\text{D})$ .

One interesting feature of our results is that they display a route to propynal in interstellar clouds. Maclagan et al.<sup>12,14</sup> have proposed that in interstellar clouds propynal may possibly form from **M1** by a dissociative electron recombination reaction, but not from the  $\text{C}_2$  protonated propadienone, **M5**. To form propynal from the most stable  $\text{C}_3\text{H}_3\text{O}^+$  isomer, **M5**, one requires a mechanism by which **M5** can rearrange to **M1**. Their results, obtained at G2//MP2/6-31G(d), indicated that any rearrangement from **M5** to **M1** would involve a TS higher in energy than  $\text{C}_2\text{H}_3^+$  (nonclassical) + CO, as **M1** is 0.65 kcal/mol less stable than these species. At the temperature of interstellar clouds, such a rearrangement would not be possible. Our CCSD(T)/cc-pVTZ//B3LYP/cc-pVTZ

calculations place **M1** 0.1 kcal/mol under  $\text{C}_2\text{H}_3^+$  (nonclassical) + CO, and provide us with a new accessible route from **M5** passing through **TS35**, **M3**, **TS23**, **M2**, and **TS12** to give **M1** (see Fig. 1), which could yield interstellar propynal.

## Thermodynamic Analysis

The results of the thermodynamic analysis of the different energy profiles performed at 100, 298.15, and 2000 K are collected in Table II. Figure 3 displays the  $\Delta G$  profile at 2000 K.

From Table II we see that when going from 100 to 298.15 K most of the structures undergo negative variations of  $\Delta H$ . Only **M3**, **TS34**, **M4**, and **TS35** present positive variations, while **M2** and the proton transfer products,  $\text{C}_2\text{H}_3^+$  (nonclassical) + CO, have the same  $\Delta H$  at both temperatures. On the contrary, when going from 100 to 2000 K, only the higher TSs, **TS15**, **TS16**, **TS67**, and **TS78**, present negative  $\Delta H$  variations.  $\Delta H$  for the reaction  $\text{HCO}^+ + \text{C}_2\text{H}_2 \rightarrow \text{C}_2\text{H}_3^+ + \text{CO}$  is −11.8, −11.8, and −11.2 kcal/mol at 100, 298.15, and 2000 K, respec-

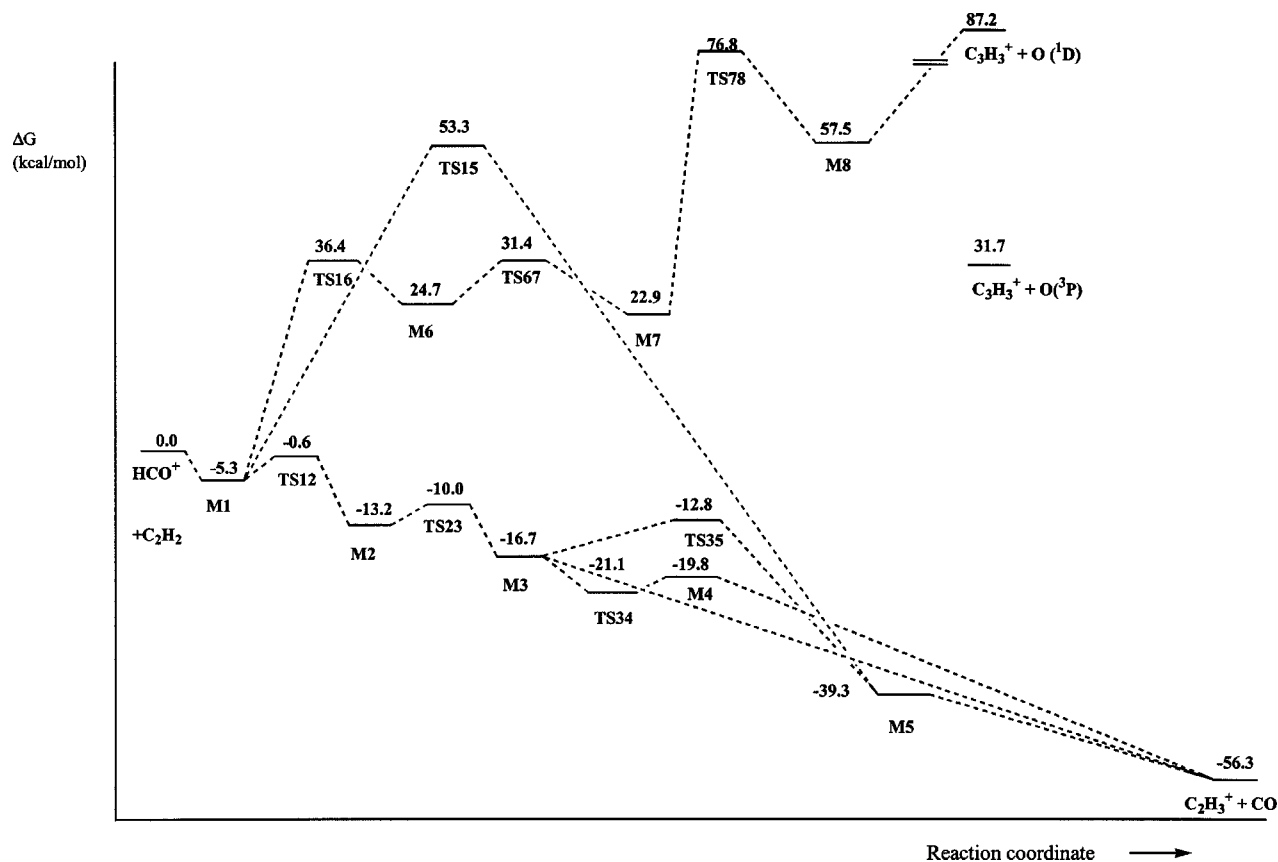


**FIGURE 3.**  $\Delta G$  profile at 2000 K for the reaction between  $\text{HCO}^+$  and  $\text{C}_2\text{H}_2$ .

tively. For the elimination of an oxygen atom in its ground state ( $^3\text{P}$ ) and the formation of  $\text{C}_3\text{H}_3^+$  from  $\text{HCO}^+$  and  $\text{C}_2\text{H}_2$ ,  $\Delta H$  is 62.3, 61.8, and 63.9 kcal/mol at 100, 298.15, and 2000 K, respectively, to compare with the reported value<sup>6</sup> of  $-67$  kcal/mol at room temperature for the reverse process.

Concerning the Gibbs energy profiles, the entropic contribution at 100 and 298.15 K destabilizes all the species relative to reactants except **TS34** and the products. At 2000 K, the entropic term stabilizes besides three other structures: **M3**, **M4**, and **TS35**. It is interesting to note that the products  $\text{C}_2\text{H}_3^+$  (nonclassical) + CO become considerably more stable than reactants with increasing temperature so that at 2000 K they are 17.0 kcal/mol more stable than **M5** and 56.3 kcal/mol more stable than separate reactants (see Fig. 3). Consequently, according to the above-mentioned Gibbs energy profile variations, one would expect that at low (interstellar chemistry) and moderate temperatures **M5** could play a certain role, whereas at high temperatures (combustion chemistry) the most thermodynamically favored species are  $\text{C}_2\text{H}_3^+$  (nonclassical) + CO products.

In summary, our CCSD(T)/cc-pVTZ//B3LYP/cc-pVTZ results display an accessible route to propynal in interstellar clouds conditions connecting the most stable  $\text{C}_3\text{H}_3\text{O}^+$  isomer with a species from which propynal may be produced in a dissociative electron recombination reaction. The reaction channel to produce  $\text{C}_3\text{H}_3^+$  (nonclassical) + O evolves basically through two energy barriers and presents an endothermicity of 63.9 kcal/mol at 2000 K. According to our Gibbs energy profiles, the C2-protonated propadienone is the most stable species at low-moderate temperatures, and consequently, could play a certain role in interstellar chemistry. On the contrary, in combustion chemistry conditions (high temperatures) the  $\text{C}_2\text{H}_3^+$  (nonclassical) + CO products are the most thermodynamically favored species.

## References

- Warnatz, J. In *Combustion Chemistry*; Gardiner, Jr., W. C., Ed.; Springer Verlag: Berlin, 1984, p. 197.
- Bohme, D. K.; Goodings, J. M.; Ng, C. W. *Int J Mass Spectrom Ion Phys* 1977, 24, 25.
- Smith, D. *Chem Rev* 1992, 92, 1473.
- Calcote, H. F. In *Ninth Int. Symp. on Combustion*; Academic Press: New York, 1963, p. 622.
- Calcote, H. F. In *Eighth Int. Symp. on Combustion*; Williams and Wilkins: Baltimore, MD, 1962.
- Calcote, H. F. In *Ion Molecule Reactions*; Franklin, J. L., Ed.; Plenum: New York, 1972, Vol. 2, p. 673.
- (a) McAllister, T.; Nicholson, A. J. C. *J Chem Soc Faraday Trans 1* 1981, 77, 821; (b) McAllister, T. *Aust J Chem Soc* 1984, 37, 511.
- Díaz, N.; Suárez, D.; Sordo, T. L. *J Phys Chem A* 1998, 102, 9918.
- López, R.; del Río, E.; Menéndez, M. I.; Sordo, T. L. *J Comput Chem*, accepted for publication.
- Vinckier, C.; Gardner, M. P.; Bayes, K. D. In *Sixteenth Int. Symp. on Combustion*; The Combustion Institute: Pittsburgh, 1977, p. 881.
- Homes, J. L.; Terlouw, J. K.; Burgers, P. C. *Organic Mass Spectrom* 1980, 15, 140.
- Scott, G. B. I.; Fairley, D. A.; Freeman, C. G.; MacLagan, R. G. A. R.; McEwan, M. J. *Int J Mass Spectrom Ion Proc* 1995, 149/150, 251.
- Bouchoux, G.; Hoppilliard, Y.; Flament, J. P. *Organic Mass Spectrom* 1985, 20, 560.
- MacLagan, R. G. A. R.; McEwan, M. J.; Scott, G. B. I. *Chem Phys Lett* 1995, 240, 185.
- Adams, N. G.; Smith, D.; Giles, K.; Herbst, E. *Astron Astrophys* 1989, 220, 269.
- Frisch, M. J.; Trucks, G. W.; Schlegel, H. B.; Gill, P. M.; Johnson, B. G.; Robb, M. A.; Cheesman, J. R.; Keith, T. A.; Petersson, G. A.; Montgomery, J. A.; Raghavachari, K.; Al-Lahan, M. A.; Zkrzewski, V. G.; Ortiz, J. V.; Foresman, J. B.; Cioslowski, J.; Stefanov, B. B.; Nanayakkara, A.; Challacombe, M.; Peng, C. Y.; Ayala, P. Y.; Chen, W.; Wong, M. W.; Andres, J. L.; Replogle, E. S.; Gomperts, R.; Martin, R. L.; Fox, D. L.; Binkley, J. S.; Defrees, D. J.; Baker, J.; Stewart, J. P.; Head-Gordon, M.; Gonzalez, C.; Pople, J. A. *Gaussian 94*; Gaussian, Inc: Pittsburgh, PA, 1995.
- Schlegel, H. B. *J Comput Chem* 1982, 3, 211.
- (a) Dunning, T. H. *J Chem Phys* 1989, 90, 1007; (b) Woon, D. E.; Dunning, T. H. *J Chem Phys* 1993, 98, 1358.
- (a) Fukui, K. *Acc Chem Res* 1981, 14, 363; (b) Gonzalez, C.; Schlegel, H. B. *J Phys Chem* 1989, 90, 2154; (c) Gonzalez, C.; Schlegel, H. B. *J Phys Chem* 1990, 94, 5523.
- Benson, S. W. In *Thermochemical Kinetics*; Wiley-Interscience: New York, 1976.
- (a) Reed, A. E.; Weinstock, R. B.; Weinhold, F. *J Chem Phys* 1985, 83, 735; (b) Reed, A. E.; Curtiss, L. A.; Weinhold, F. *Chem Rev* 1988, 88, 899.